THE JOURNAL OF PHYSICAL CHEMISTRY B

ARTICLE

pubs.acs.org/JPCB

Linear and Nonlinear Optical Properties of the Thiophene/Phenylene-Based Oligomer and Polymer

M. G. Vivas,[†] S. L. Nogueira,[‡] H. Santos Silva,[‡] N. M. Barbosa Neto,[‡] A. Marletta,[‡] F. Serein-Spirau,[§] S. Lois,[§] T. Jarrosson,[§] L. De Boni,[†] R. A. Silva,[‡] and C. R. Mendonca*[,†]

[†]Instituto de Física de São Carlos, Universidade de São Paulo, São Carlos, Brazil

[‡]Instituto de Física, Universidade Federal de Uberlândia, MG, Brazil

[§]Institut Charles Gerhardt, Equipe AM_2N, Architectures Moléculaires et Matériaux Nanostructurés, ENSCM, Montpellier, France

ABSTRACT:

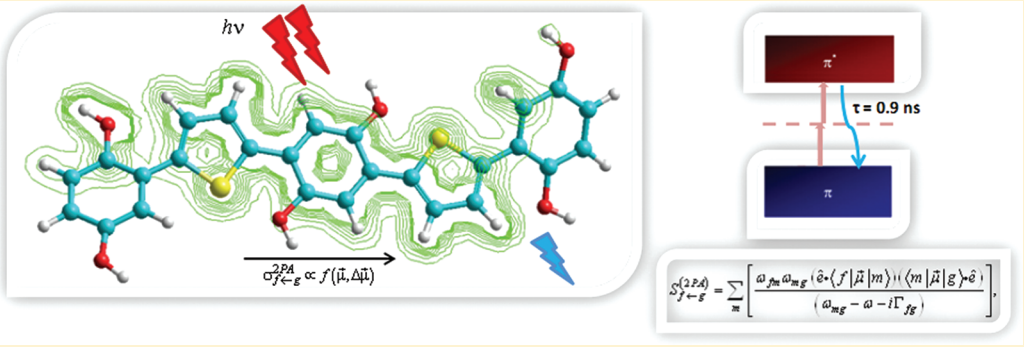

In this article, we investigate the linear and nonlinear optical properties of the thiophene/phenylene-based oligomer (SL128G) and polymer (FSE59) chemically modified with alquilic chains, which allow greater solubility and provide new optical properties. These compounds present a strong absorption in the UV−visible region, providing a wide transparence window in visible-IR, ideal for applications in nonlinear optics. Employing the Z-scan technique with femtosecond pulses, we show that these compounds exhibit considerable two-photon absorption (2PA), with two 2PA allowed states located at 650 and 800 nm for SL128G and 780 and 920 nm for FSE59. Moreover, we observe the resonance enhancement effect as the excitation wavelength approaches the lowest one-photon-allowed state. By modeling the 2PA spectra considering a four-energy-level diagram within of the sum-over-essential states approach, we obtained the spectroscopic parameters of the electronic transitions to low-energy singlet excited states. Additionally, photoluminescence excited by femtosecond and picosecond pulses were performed to confirm the order of the multiphoton process and estimate the fluorescence lifetime, respectively.

1. INTRODUCTION

Conjugated organic molecules have attracted considerable attention in the last decades due to their remarkable optoelectronic properties.[1−5] Their structural malleability allows tunable optical properties, which can be exploited for different applications. The thiophene- and phenylene-based oligomers and polymers constitute an important class of organic molecules that exhibit a high degree of electronic delocalization as well as optical tunability, essential to optoelectronic and photonic devices. In addition, these materials stand out due to the combination of their excellent film-forming properties with interesting absorption and light-emitting ability.[6] However, they present low solubility in organic solvents at room temperature. To circumvent this limitation, a new class of thiophene/phenylene-based oligomer and polymer in which alquilic chains were introduced in the 2 and 5 positions of the phenylene group were synthesized. Besides increasing the solubility, the alquilic chains provide new properties such as photo- and thermal-stability.[6]

Conjugated polymers derive their semiconducting properties from the π-electron delocalization along the polymer chain. The π (bonding) and π^* (antibonding) orbitals form delocalized valence and conduction wave functions, which support mobile charge carriers. Therefore, thiophene/phenylene-based polymers present high electronic delocalization due to their π-conjugated structure, essential to applications involving nonlinear optical processes. Among these effects, the two-photon absorption (2PA) has drawn attention because of its quadratic dependence with the irradiance, which allows high spatial localization of the excitation.[7] This characteristic provides a wide range of applications such as optical power limiting,[8] two-photon fluorescence microscopy,[9] photopolymerization via two-photon absorption,[10−12] three-dimensional optical storage memory,[13,14] and photodynamic therapy.[15] In this

Received: April 6, 2011
Revised: October 3, 2011
Published: October 04, 2011

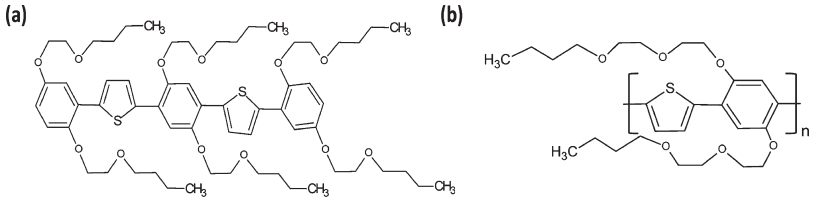

Figure 1. Molecular structures of (a) SL128G and (b) FSE59.

Table 1. Photophysical Parameters of the SL128G and FSE59 Studied Here

molecule	states	λ_{max}^{abs} (nm)	λ_{max}^{emi} (nm)	Stokes shift (cm^{-1})	φ_f	τ_{10} (ps)	bandgap (eV)	$\sigma_{f\leftarrow g}^{(2PA)}$ (GM)
SL128G	S_1	405	457	2809	0.71	930	2.73	55
	S_2	330						245
	S_3	270						585
FSE59	S_1	470	521	2083	0.79	870	2.39	125
	S_2	400						650
	S_3	320						2250

type of process, the chromophore simultaneously absorbs two photons of longer wavelength, whose sum in energy is sufficient to promote the electronic transition analogue the absorption of a single photon with a shorter wavelength.

Several papers have investigated the nonlinear optical properties of oligomers, polymers, and dendrimers[16−20] employing different techniques.[21−25] However, only a few studies have reported a broadband analysis using femtosecond pulses with a low repetition rate. The short pulse duration allows obtaining pure 2PA because only negligible absorption comes from the population generated in the excited states, while the low repetition rate (1 kHz) helps to avoid cumulative thermal effects that can produce a thermo-optical distortion. In this context, we investigate the nonlinear optical properties of the thiophene/phenylene-based oligomer (SL128G) and polymer (FSE59), chemically modified with alquilic chains, using the Z-scan technique with femtosecond pulses at a low repetition rate. The nonlinear spectra were modeled using the sum-over-essential states approach[26,27] with a four-energy-level diagram (ground state and three excited states). In recent years, two-photon absorption spectroscopy has proved to be a powerful tool to estimate molecular parameters of organic compounds.[28] Finally, to confirm the order of multiphoton processes observed, we measured the intensity of excited fluorescence via femtosecond pulses as a function of irradiance. Moreover, we report the linear optical properties such as, one-photon absorption cross-section, one-photon induced fluorescence, fluorescence quantum yield, and lifetimes.

2. EXPERIMENTAL AND 2PA APPROACH

2.1. Compounds. The compounds SL128G and FSE59, whose molecular structures are illustrated in Figure 1a and b, respectively, were synthesized according to the scheme employed by Stille[29] and Miyaura−Suzuki.[30] Using this methodology, we obtained a reaction yield of approximately 90% for both compounds. The oligomer presents five aromatic rings, while the degree of polymerization obtained by gel permeation chromatography (GPC) indicates an average number of 25−30 consecutive aromatic rings in the polymeric chain. The fluorescence quantum yield (φ_f) of SL128G and FSE59 was obtained by the Williams method,[31] and the results are shown in Table 1.

2.2. Optical Measurements. We prepared thiophene/phenylene/tetrahydrofuran (THF) (SL128G and FSE59) solutions with concentrations around at 10 $mg \cdot L^{-1}$ and 1 $g \cdot L^{-1}$, for linear and nonlinear optical measurements, respectively. The samples were placed in a 2 mm thick quartz cuvette for optical measurements. The linear absorption spectrum and photoluminescence spectrum were recorded using a Cary 17 spectrophotometer and a Perkin-Elmer LS55 fluorimeter, respectively. Nonlinear optical measurements were carried out employing the open aperture Z-scan technique,[21] using 120 fs laser pulses from an optical parametric amplifier pumped by 150 fs pulses at 775 nm, delivered by a Ti/sapphire chirped pulse amplified system, operating at a 1 kHz repetition rate. The Z-scan measurements were carried out with intensities ranging from 50 to 200 GW/cm^2 (15 to 130 nJ/pulse), with a beam waist size ranging from 14 to 22 μm. The same laser system was used to excite the sample's fluorescence, which was collected perpendicularly to the excitation through an optical fiber attached to a spectrometer. The fluorescence intensity as a function of the excitation irradiance was measured at 640 and 780 nm, close to the most intense 2PA band for the oligomer and polymer, respectively.

For an absorptive nonlinearity, the light field induces an intensity dependent absorption coefficient, $\alpha = \alpha_0 + \beta I$, where I is the laser beam intensity, α_0 is the linear absorption coefficient, and β is the 2PA coefficient. After carrying out the open aperture measurement, the nonlinear absorption coefficient can be unambiguously determined by fitting the experimental data.[32] The 2PA cross-section can be obtained through the expression $\sigma^{(2PA)} = \hbar\omega\beta/N$, where N is the number of molecules per cm^3, and $\hbar\omega$ is the photon energy.

To measure the fluorescence lifetime of the samples, we used the second harmonic of a Q-switched and mode-locked Nd:YAG laser with 70 ps of pulse duration. The second harmonic is focused in a BBO (beta barium borate) crystal to generate 266 nm. The 266 nm beam was focused into the sample with a lens of focal length $f = 12$ cm. The sample was placed in a 2 mm thick fused silica cuvette. The fluorescence signal was collected perpendicularly to the excitation beam by an optical fiber positioned close to the fluorescent spot. The signal was acquired by a silicon photodetector with a rise time of approximately 0.5 ns and subsequently averaged and recorded with a digital oscilloscope (5 GS/s). The fluorescence lifetime is determined by the deconvolution of the decay curves and subsequent fitting using exponential functions. With this system, we are limited to measure lifetimes higher than 0.5 ns with a typical accuracy of approximately 0.1 ns, obtained by the standard deviation of the mean lifetime, determined by repeating the experiment several times. Excitation at the magic angle was not used because we do not have resolution to observed rotation contributions.

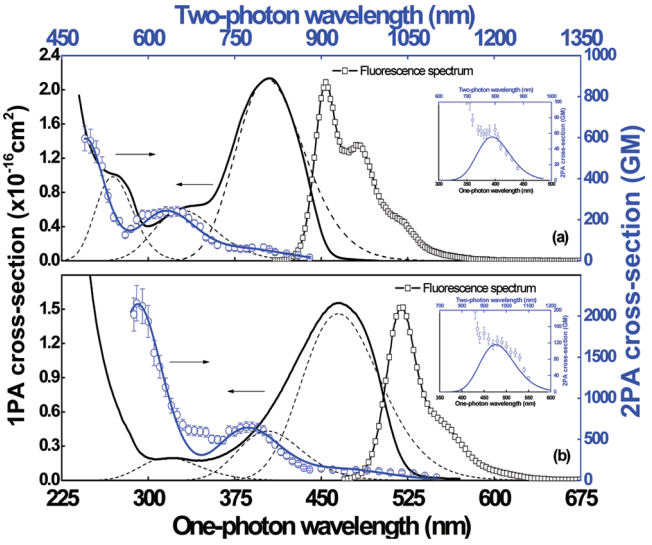

Figure 2. (a) SL128G and (b) FSE59. The solid lines and squares show the linear absorption and fluorescence spectra, respectively. The dashed lines represent the Gaussian superposition of the 1PA spectrum, while circles represent the 2PA spectra with the solid line being the theoretical fit obtained with the sum-over-essential states approach. The insets show the zoom of the lowest energy 2PA band, while the solid lines represent the weakly 2PA allowed transition described by the first term of eq 3.

We consider that in our detection window all rotation diffusion has already taken place and that the fluorescence we are measuring refers only to a random distribution of fluorophores.

2.3. Sum-over-Essential States Approach for 2PA. The 2PA cross-section can be obtained by the semiclassical time-dependent perturbation theory. In this approach, the two-photon absorption cross-section can be evaluated via second-order transition matrix elements, given by the following:

$$S_{f\leftarrow g}^{(2PA)} = \sum_m \left[\frac{\omega_{fm}\omega_{mg}(\hat{e}\cdot\langle f|\vec{\mu}|m\rangle)(\langle m|\vec{\mu}|g\rangle\cdot\hat{e})}{(\omega_{mg}-\omega-i\Gamma_{fg})}\right] \quad (1)$$

where $\vec{\mu}$ is the dipole moment vector, Γ_{fg} is the damping constant describing full width at half-maximum of the final state line width (assuming Gaussian line-shape), $\omega_{f\leftarrow g}$ is the transition frequency, and $\hat{e} = \vec{e}/e$ is the vector that describes the light polarization direction. The summation represents the sum over all real electronic states, i.e., the initial ($|g\rangle$), intermediates ($|m\rangle$), and final ($|f\rangle$) states. The 2PA cross-section, following the methodology described in the ref 33, can be written in the cgs system of units, as follows:

$$\sigma_{f\leftarrow g}^{(2PA)} = 4\frac{(2\pi)^5}{(nhc)^2}L^4\omega^2\left|\sum_m\left[\frac{(\hat{e}\cdot\vec{\mu}_{fm})(\vec{\mu}_{mg}\cdot\hat{e})}{[(\omega_{fg}-\omega)-i\Gamma_{fg}(\omega)]}\right]\right|^2 g_{f\leftarrow g}(2\omega) \quad (2)$$

where h is Planck's constant, c is the speed of light, ω is the excitation laser frequency, $L = (n^2+2)/3$ is the Lorentz local field factor introduced to take into account the effect media[34] with $n = 1.40$ (refractive index) for THF, and $g(2\omega)$ represents the line width function.

Many molecules, including those studied here, do not present a center of inversion and, therefore, initial and final states have a static dipole moment. Thus, it is necessary to take into account the intermediate energy levels. In addition, noncentrosymmetric molecules do not follow the dipole−electric selection rule,[35] and therefore, one- and two-photon transitions are allowed between any levels. In this case, taking into account the average over all possible molecular orientations in an isotropic medium and considering that only one intermediate state, $|1\rangle$ (one- and two-photon-allowed), contributes significantly to the transition matrix elements, the 2PA cross-section can be written as follows (assuming linearly polarized light and that the dipole moments are parallel):

$$\begin{aligned}\sigma_{f\leftarrow g}^{(2PA)}(\omega) = {} & \frac{4}{5}\frac{(2\pi)^5}{(nhc)^2}L^4\omega^2\left\{\frac{|\vec{\mu}_{01}|^2|\Delta\vec{\mu}_{01}|^2}{\omega^2}\right.\\ & + \frac{1}{(\omega_{01}-\omega)^2+\Gamma_{01}{}^2(\omega)}|\vec{\mu}_{01}|^2[|\vec{\mu}_{12}|^2+|\vec{\mu}_{13}|^2]\\ & + \frac{2(\omega_{01}-\omega)^2}{(\omega_{01}-\omega)^2+\Gamma_{01}{}^2(\omega)}|\vec{\mu}_{01}|^2\left[\frac{|\Delta\vec{\mu}_{01}||\vec{\mu}_{12}|}{\omega(\omega_{01}-\omega)}\right.\\ & \left.\left.+\frac{|\Delta\vec{\mu}_{01}||\vec{\mu}_{23}|}{\omega(\omega_{01}-\omega)}+\frac{|\vec{\mu}_{12}||\vec{\mu}_{23}|}{(\omega_{01}-\omega)^2+\Gamma_{01}{}^2(\omega)}\right]\right\}g_{f\leftarrow g}(2\omega)\end{aligned} \quad (3)$$

where $\Delta\vec{\mu}_{01}$ is the difference between the permanent dipole moments in the excited ($\vec{\mu}_{11}$) and ground ($\vec{\mu}_{00}$) states. The following additional simplifications were used: $\omega_{fg}-\omega \gg \Gamma_{fg}$, and $\omega_{fg}-\omega = \omega$, since the final energy level is never in close resonance with the excitation photons in a degenerate 2PA process.[36] As can be seen from eq 3, the 2PA cross-section is governed by three contributions: the first corresponds to a 2PA transition in a two-level system with a change of permanent dipole moment, while the second contribution corresponds to the transition in a four-level system with two final states, $|2\rangle$ and $|3\rangle$, and one intermediate real state ($|1\rangle$), which contribute to the resonance enhancement of the nonlinearity. The last contribution corresponds to an interference between the three excited states. Such a term can contribute positively or negatively to the 2PA cross-section, depending on the spectral region.

3. RESULTS AND DISCUSSION

The linear absorption spectra of SL128G and FSE59 in THF solutions are illustrated in Figure 2a,b (solid line), respectively. Such spectra present a lowest energy absorption band between 350 and 460 nm for SL128G and 380−530 nm for FSE59 with 1PA cross-section magnitude in the order of 10^{-16} cm^2. It is observed that the FSE59 presents a significant bathochromic shift in the absorption (about 60 nm or 3500 cm^{-1}) with respect to SL128G due to the increase in the number of repeating units.

In Figure 2, the squares represent the photoluminescence (PL) spectra excited at the maxima of the linear absorption. Such spectra present a strong emission band from 415 to 585 nm for SL128G and from 470 to 640 nm for FSE59, which exhibited well-defined vibronic progressions with peaks between the 0−0 and 0−1 transitions separated by 1400 cm^{-1} (~170 meV) in both molecules, consistent with the C=C stretch vibrational mode.[37] In addition, the PL spectra present maximum peaks at 521 nm for FSE59 and 457 nm for SL128G, indicating a bathochromic shift of the polymer of c.a. 64 nm (~2700 cm^{-1}), analogue to the absorption. The Stokes shift calculated for both compounds are 2809 cm^{-1} and 2083 cm^{-1} for SL128G and FSE59, respectively.

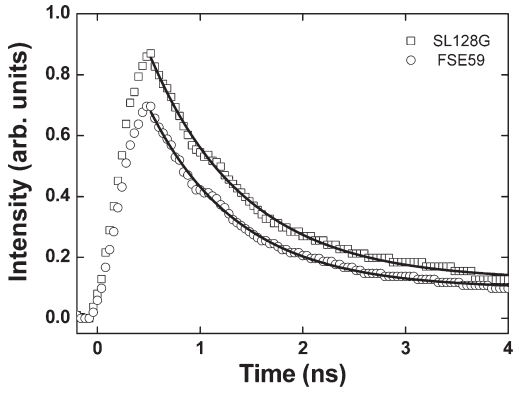

Figure 3. Time-resolved fluorescence for SL128G (squares) and FSE59 (circles) obtained using picosecond excitation at 266 nm. The fluorescence lifetimes, 0.9 ± 0.1 ns, were determined through the deconvolution method.

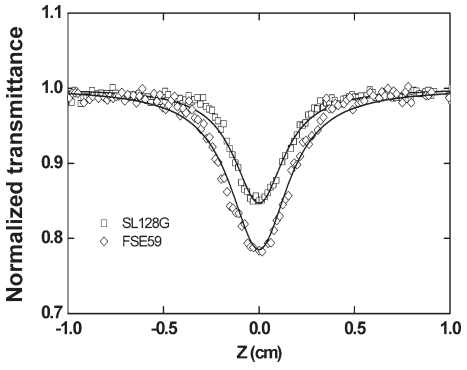

Figure 4. Open-aperture Z-scan curves for SL128G (squares) and FSE59 (diamond) in THF at 640 and 780 nm, respectively. The solid line represents the fitting employing the theory described in ref 32.

These low values indicate the high radiative emission, confirmed by measurements of the quantum fluorescence yield (see Table 1).

We measured the fluorescence lifetime for both compounds using picosecond pulses at 266 nm. Figure 3 shows the deconvoluted fluorescence decay signals for SL128G (squares) and FSE59 (circles) as well as the lifetime values obtained by fitting the data with a monoexponential function. Considering our experimental error, both compounds present a lifetime of 0.9 ± 0.1 ns. These values are in good agreement with those obtained for oligomers and polymers with a similar structure.[16,38,39]

The circles in Figure 2 represent the two-photon absorption cross-section spectra determined by open-aperture Z-scan measurements,[21] similar to the ones presented in Figure 4. The decrease observed in the normalized transmittance as a function of the *z*-position indicates a 2PA process since excitation took place in nonresonant conditions.

The nonlinear spectra (circles in Figure 2) present the resonance enhancement effect as the excitation frequency approaches the one-photon-allowed lowest energy state and two 2PA bands centered at approximately 650 and 800 nm for SL128G and 780 and 920 nm for FSE59. These bands correspond to a transition to an energy state located at the UV−visible region, accomplished by the absorption of two-photons in the visible and near-infrared. It is important to note that the 2PA spectrum of FSE59 presents a bathochromic shift of approximately

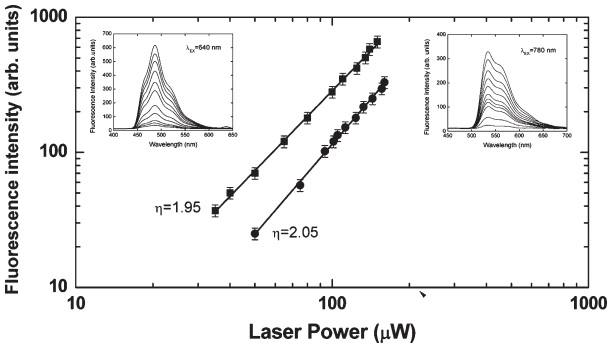

Figure 5. Photoluminescence measurements (log−log scale) as a function of laser power that show the slope of approximately 2.0 at 640 and 780 nm excitation wavelengths, respectively, for SL128G (squares) and FSE59 (circles). These results confirm the two-photon nature of the nonlinear process.

3200 cm^{-1} in relation to SL128G, which is in good agreement with the shift observed in the linear absorption. The cross-section values, at the peak of the 2PA bands, were determined to be c.a. 245 ± 25 GM at 650 nm and 55 ± 10 GM at 800 nm for SL128G; and 650 ± 65 GM at 780 nm and 125 ± 15 GM at 920 nm for FSE59 (see Table 1). In the resonance enhancement region, both compounds present high 2PA cross-section around of 585 ± 60 GM at 500 nm for SL128G and 2250 ± 225 GM at 600 nm for FSE59.

The 2PA cross-section obtained for compounds with molecular structures similar to the thiophene/phenylene oligomer has shown values in the order of hundreds of GM, close to the ones we report here.[40,41] Even though the one- and two-photon selection rules are distinct for centrosymmetric molecules, we observed that all one-photon-allowed states are also two-photon-allowed due to the relaxation of the parity selection rules[42] for noncentrosymmetric molecules, such as the ones studied here.

The insets of Figure 2 show details of the lowest-energy 2PA band for both compounds. We observed that the monotonous decrease of the 2PA band, related to the $S_0 \rightarrow S_2$ transition, is interrupted by an increase in the 2PA cross-section when the excitation photons approach the $S_0 \rightarrow S_1$ transition, indicating that there is a 2PA allowed state in this region. However, as reported by Jonhsen et.al.,[16] there is a structure loss in the 2PA band with the increase in conjugation length, accomplished by an increase in the magnitude of the 2PA cross-section.

Although the magnitude of the 2PA cross-section per repeat unit for FSE59 is approximately 2.5 times higher than that for SL128G, the 2PA cross-section per chromophore is about 45% smaller. That is probably related to the smaller planarity of the ground-state equilibrium geometry of FSE59 due to the chain folding.[43] Furthermore, according to S. Lois,[44] the oligomer studied here presents a noncovalent interaction between the oxygen and sulfur, attributed to the stiffness of their molecular structure in solution. Such an effect decreases the interaction between the chains and avoids losses of energy by the non-radiative process. The polymer also presents this effect but with smaller magnitude due to an increase in the torsion of the dihedral angle caused by growth of the polymeric chain, corroborating our experimental results.

In Figure 5, we show the quadratic dependence observed for the fluorescence intensity as a function of the excitation laser irradiance at 640 and 780 nm, close to the most intense 2PA band

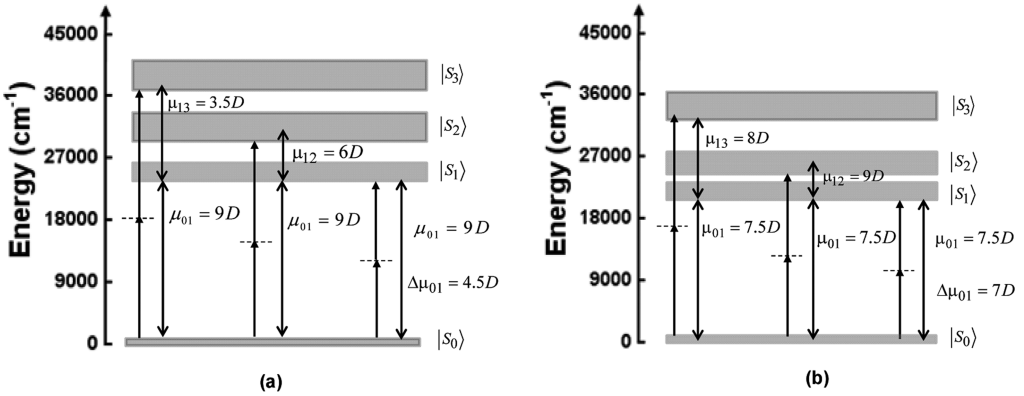

Figure 6. (a) SL128G and (b) FSE59. Four-energy-level representative diagram used to describe the 2PA cross-section spectra under the sum-over-essential states approach.

for SL128G and FSE59, respectively. It is well-known that the slope derived from a linear fit (log−log scale) of the photoluminescence intensity as a function of excitation intensity indicates the mechanism of absorption in the material.[45] In Figure 5, the insets show the fluorescence spectra excited by femtosecond pulses. A small difference is observed between the fluorescence spectra excited by 2PA and the one excited by one-photon (shown in Figure 2), which is due to an excited state reabsorption.

In order to better understand the 2PA spectrum and its connection with the molecular properties of the compounds, we employed the sum-over-essential states approach described in section 2.3. To model the 2PA spectra of the compounds, we considered the four-energy-level diagram shown in Figure 6, based on the excited states energies, obtained from the two-photon absorption spectra. However, most of the spectroscopic parameters used in this model (sum-over-essential states) can be obtained from the linear absorption spectra, such as the one-photon-allowed states and the damping factor. In this way, we fit the linear absorption spectra considering the same energy diagram showed in Figure 6, assuming that the absorption bands of the compounds investigated exhibit a Gaussian line-shape given by the following:[46]

$$g_{f\leftarrow g}(\omega) = \sqrt{\frac{4\ln(2)}{\pi\Gamma_{f\leftarrow g}{}^2}}\exp\left[-\frac{4\ln(2)}{\Gamma_{fg}{}^2}(\omega_{f\leftarrow g}-\omega)^2\right] \quad (4)$$

with absorption maxima at 270 nm (Γ_{03} = 5340 cm^{-1} = 0.66 eV), 330 nm (Γ_{02} = 5500 cm^{-1} = 0.68 eV), and 405 nm (Γ_{01} = 4330 cm^{-1} = 0.54 eV) for SL128G; and 320 nm (Γ_{03} = 5000 cm^{-1} = 0.62 eV), 400 nm (Γ_{02} = 4340 cm^{-1} = 0.54 eV), and 470 nm (Γ_{01} = 4000 cm^{-1} = 0.5 eV) for FSE59, as shown by dashed lines in Figure 2. Oligomers with similar molecular structure, such as vinylene-phenylene, thiophene analogues, and vinylene-thiophene, also possess electronic transitions with considerable oscillator strengths in these regions, which also are populated by the 2PA process.[16,47,48] Additionally, to reduce the number of adjustable parameters, a complementary analysis was performed to determine the transition dipole moments of the compounds using the linear absorption spectra. From the first-excited state absorption, we can calculate the transition dipole moment of the transition from the ground to the first-excited states using[49]

$$\mu_{f\leftarrow g} = \sqrt{\frac{3}{4\pi}\frac{c}{\pi^{1/2}}\sigma_{1PA}^{max}\frac{\Gamma_{f\leftarrow g}}{2(\ln(2))^{1/2}}\frac{h}{\omega_{f\leftarrow g}}} \quad (5)$$

Table 2. Spectroscopic Parameters Used and Obtained in the Sum-over-Essential States Approach, Employing the Four-Energy-Level Diagram[a]

2PA parameters	SL128G	FSE59
ν_{01} (cm^{-1})	25350 (395 nm)	21280 (470 nm)
ν_{02} (cm^{-1})	30690 (325 nm)	25350 (395 nm)
ν_{03} (cm^{-1})	40000 (250 nm)	33356 (300 nm)
Γ_{01} (cm^{-1})	4330 ± 500	4000 ± 500
Γ_{02} (cm^{-1})	5500 ± 500	4340 ± 500
Γ_{03} (cm^{-1})	5340 ± 500	5000 ± 500
μ_{01} (Debye)	9.0 ± 0.5	7.5 ± 0.5
μ_{12} (Debye)	6.0 ± 1	9.0 ± 1
μ_{13} (Debye)	3.5 ± 0.5	8.0 ± 1
$\Delta\mu_{01}$ (Debye)	4.5 ± 0.5	7.0 ± 1

[a] Γ is the damping constant describing the full width at half-maximum of the final state linewidth, and $\nu_{fg} = \omega_{fg}/2\pi$.

where σ_{1PA}^{max} is the maximum one-photon absorption cross-section in cm^2. The value obtained from eq 2 is expressed in Debye.

The solid line along the circles in Figure 2 represents the fitting assuming Gaussian line-shapes obtained using eq 3 with ω_{01}, ω_{02}, and ω_{03} taken from the 2PA absorption spectrum (bands located at 395, 325, and 250 nm for SL128G and 470, 395, and 300 nm for FSE59). The damping constant describing the full width at half-maximum of the final state line width and transition dipole moment (μ_{01}) were estimated from eqs 4 and 5, respectively. The peak positions of the 2PA bands are shifted by about 900 cm^{-1} with respect to the linear absorption peak, probably due to the distinct vibronic coupling between one- and two-photon transitions.[27] From the 2PA fitting, we were able to estimate $\Delta\mu_{01}$, μ_{12}, and μ_{13} for both compounds. Table 2 summarizes the spectroscopic parameters used/obtained in the sum-over-essential states approach used to model the 2PA spectra.

The transition dipole moment between the ground and excited states for both compounds are very close to each other, being slightly higher for SL128G. However, the magnitude of the dipole moment between the excited states ($|S_1\rangle \rightarrow |S_2\rangle$ and $|S_1\rangle \rightarrow |S_3\rangle$) are higher for FSE59, probably due to its larger conjugation length. We also observe that both compounds present a moderate permanent dipole moment change associated with the lowest 2PA allowed transition, which is governed by the first term of eq 3. The solid lines shown in the inset of Figure 2

represent this weakly allowed 2PA band, with $\Delta\mu_{01} = 4.5D$ for SL128G and $\Delta\mu_{01} = 7.0D$ for FSE59.

Finally, we observed that as the conjugation length increases, as in FSE59, the 2PA spectrum presents a red-shift corresponding to a decrease in the energy of the two-photon-allowed states, as shown in Figure 6, concomitantly increasing the 2PA cross-section. This decrease in energy (small band gap) favors the contribution of the 2PA allowed intermediate energy level, providing a significant resonance enhancement of the 2PA cross-section of approximately 18 times (against 10 times for SL128G) in comparison to its dipolar transition, which does not involve any intermediate states. The effect of the extent of the conjugation length on the multiphoton absorption process, as well as on the resonance enhancement effect in organic compounds, has been investigated in the last years.[16,40,50−52]

4. CONCLUSIONS

We reported the linear and nonlinear optical properties of thiophene/phenylene derivatives, which are organic compounds with noteworthy features for technological applications. The linear optical properties, including absorption and one-photon-induced fluorescence, fluorescence quantum yield, and lifetimes were reported. Besides, the 2PA absorption spectra were investigated using femtosecond laser pulses and low repetition rate. We observed that both compounds present high 2PA cross-sections associated with the resonance enhancement effect, as well as two bands corresponding to transitions to singlet excited states in the UV−visible region. These transitions are two-photon-allowed because of the relaxation of the parity selection rules for some noncentrosymmetric molecules. We have confirmed the order of nonlinear processes using an up-conversion fluorescence measurement with femtosecond pulses. Transition dipole moments between the ground and excited states and between singlet-excited states, as well as permanent dipole moment change, which are directly related to the photochemical properties of these compounds, were obtained by fitting the linear and two-photon absorption spectra using the Gaussian line-shape. From a technological point of view, the results presented in this study can guide the development of 2PA-based applications using these materials and their derivatives in the visible and near-infrared regions.

■ ACKNOWLEDGMENT

Financial support was from FAPESP (Fundação de Amparo à Pesquisa do estado de São Paulo), CNPq (Conselho Nacional de Desenvolvimento Científico e Tecnológico), and Coordenação de Aperfeiçoamento de Pessoal de Nível Superior (CAPES).

■ REFERENCES

(1) Ambrosio, A.; Orabona, E.; Maddalena, P.; Camposeo, A.; Polo, M.; Neves, A. A. R.; Pisignano, D.; Carella, A.; Borbone, F.; Roviello, A. *Appl. Phys. Lett.* **2009**, *94*, 011115.

(2) Correa, D. S.; De Boni, L.; Balogh, D. T.; Mendonca, C. R. *Adv. Mater.* **2007**, *19*, 2653–2656.

(3) De Boni, L.; Andrade, A. A.; Yamaki, S. B.; Misoguti, L.; Zilio, S. C.; Atvars, T. D. Z.; Mendonca, C. R. *Chem. Phys. Lett.* **2008**, *463*, 360–363.

(4) Gindre, D.; Boeglin, A.; Fort, A.; Mager, L.; Dorkenoo, K. D. *Opt. Express* **2006**, *14*, 9896–9901.

(5) Kishida, H.; Hirota, K.; Okamoto, H.; Kokubo, H.; Yamamoto, T. *Synth. Met.* **2009**, *159*, 868–870.

(6) Silva, R. A.; Cury, L. A.; Guimarães, P. S. S.; Marletta, A.; SereinpSpirau, F.; Bouachrine, M.; Moreau, J. J. E.; Lè Re-Porte, J.-P. *J. Polym. Sci., Part B: Polym. Phys.* **2010**, *48*, 964–971.

(7) Albota, M.; Beljonne, D.; Bredas, J. L.; Ehrlich, J. E.; Fu, J. Y.; Heikal, A. A.; Hess, S. E.; Kogej, T.; Levin, M. D.; Marder, S. R.; et al. *Science* **1998**, *281*, 1653–1656.

(8) Fuks-Janczarek, I.; Ebothe, J.; Miedzinski, R.; Gabanski, R.; Reshak, A. H.; Lapkowski, M.; Motyka, R.; Kityk, I. V.; Suwinski, J. *Laser Phys.* **2008**, *18*, 1056–1069.

(9) Skala, M. C.; Squirrell, J. M.; Vrotsos, K. M.; Eickhoff, V. C.; Gendron-Fitzpatrick, A.; Eliceiri, K. W.; Ramanujam, N. *Cancer Res.* **2005**, *65*, 1180–1186.

(10) Belfield, K. D.; Schafer, K. J.; Liu, Y. U.; Liu, J.; Ren, X. B.; Van Stryland, E. W. *J. Phys. Org. Chem.* **2000**, *13*, 837–849.

(11) Correa, D. S.; Tayalia, P.; Cosendey, G.; dos Santos, D. S.; Aroca, R. F.; Mazur, E.; Mendonca, C. R. *J. Nanosci. Nanotechnol.* **2009**, *9*, 5845–5849.

(12) Mendonca, C. R.; Correa, D. S.; Marlow, F.; Voss, T.; Tayalia, P.; Mazur, E. *Appl. Phys. Lett.* **2009**, *95*, 113309.

(13) Parthenopoulos, D. A.; Rentzepis, P. M. *Science* **1989**, *245*, 843–845.

(14) Mendonca, C. R.; Neves, U. M.; De Boni, L.; Andrade, A. A.; dos Santos, D. S.; Pavinatto, F. J.; Zilio, S. C.; Misoguti, L.; Oliveira, O. N. *Opt. Commun.* **2007**, *273*, 435–440.

(15) Gao, D.; Agayan, R. R.; Xu, H.; Philbert, M. A.; Kopelman, R. *Nano Lett.* **2006**, *6*, 2383–2386.

(16) Johnsen, M.; Paterson, M. J.; Arnbjerg, J.; Christiansen, O.; Nielsen, C. B.; Jørgensenb, M.; Ogilby, P. R. *Phys. Chem. Chem. Phys.* **2008**, *10*, 1177–1191.

(17) Corredor, C. C.; Huang, Z. L.; Belfield, K. D.; Morales, A. R.; Bondar, M. V. *Chem. Mater.* **2007**, *19*, 5165–5173.

(18) De Boni, L.; Andrade, A. A.; Correa, D. S.; Balogh, D. T.; Zilio, S. C.; Misoguti, L.; Mendonca, C. R. *J. Phys. Chem. B* **2004**, *108*, 5221–5224.

(19) Drobizhev, M.; Karotki, A.; Dzenis, Y.; Rebane, A.; Suo, Z.; Spangler, C. W. *J. Phys. Chem. B* **2003**, *107*, 7540–7543.

(20) Tsiminis, G.; Ribierre, J. C.; Ruseckas, A.; Barcena, H. S.; Richards, G. J.; Turnbull, G. A.; Burn, P. L.; Samuel, I. D. W. *Adv. Mater.* **2008**, *20*, 1940–1944.

(21) Sheik-Bahae, M.; Said, A. A.; Wei, T.-H.; Hagan, D. J.; Stryland, E. W. V. *IEEE J. Quantum Electron.* **1990**, *26*, 760–769.

(22) De Boni, L.; Andrade, A. A.; Misoguti, L.; Mendonca, C. R.; Zilio, S. C. *Opt. Exp.* **2004**, *12*, 3921–3927.

(23) Fakis, M.; Polyzos, I.; Tsigaridas, G.; Giannetas, V.; Persephonis, P. *Chem. Phys. Lett.* **2004**, *394*, 372–376.

(24) Bosma, W. B.; Mukamel, S.; Greene, B. I.; Schmitt-Rink, S. *Phys. Rev. Lett.* **1992**, *68*, 2456–2459.

(25) Tomov, I. V.; VanWonterghem, B.; Dvornikov, A. S.; Dutton, T. E.; Rentzepis, P. M. *J. Opt. Soc. Am. B* **1991**, *8*, 1477–1482.

(26) Birge, R. R.; Pierce, B. M. *J. Chem. Phys.* **1979**, *70*, 165–178.

(27) Kamada, K.; Ohta, K.; Iwase, Y.; Kondo, K. *Chem. Phys. Lett.* **2003**, *372*, 386–393.

(28) Rebane, A.; Drobizhev, M.; Makarov, N. S.; Beuerman, E.; Haley, J. E.; Douglas, M. K.; Burke, A. R.; Flikkema, J. L.; Cooper, T. M. *J. Phys. Chem. A* **2011**, *115*, 4255–4262.

(29) Stille, J. K. *Angew. Chem., Int. Ed.* **1986**, *25*, 508–524.

(30) Miyaura, N.; Suzuki, A. *Chem. Rev.* **1995**, *95*, 2457–2483.

(31) Dawson, W. R.; Windsor, M. W. *J. Phys. Chem.* **1968**, *72*, 3251–3260.

(32) He, G. S.; Tan, L. S.; Zheng, Q.; Prasad, P. N. *Chem. Rev.* **2008**, *108*, 1245–1330.

(33) Lim, E. C. *Excited States*; Academic Press: New York, 1977.

(34) Zhu, L. Y.; Yi, Y. P.; Shuai, Z. G.; Bredas, J. L.; Beljonne, D.; Zojer, E. *J. Chem. Phys.* **2006**, *125*, 044101.

(35) Bonin, K. D.; McIlrath, T. J. *J. Opt. Soc. Am. B* **1984**, *1*, 52–55.

(36) Meath, W. J.; Power, E. A. *J. Phys. B: At., Mol. Opt. Phys.* **1984**, *17*, 763–781.

(37) Silva, R. A.; Cury, L. A.; Marletta, A.; Guimaraes, P. S. S.; Bouachrine, M.; Lere-Porte, J. P.; Moreau, J. E.; Serein-Spirau, F. *J. Non-Cryst. Solids* **2006**, *352*, 3685–3688.

(38) Chosrovian, H.; Rentsch, S.; Grebner, D.; Dahm, D. U.; Birckner, E.; Naarmann, H. *Synth. Met.* **1993**, *60*, 23–26.
(39) de Melo, J. S.; Burrows, H. D.; Svensson, M.; Andersson, M. R.; Monkman, A. P. *J. Chem. Phys.* **2003**, *118*, 1550–1556.
(40) Nguyen, K. A.; Day, P. N.; Pachter, R. *Theor. Chem. Acc.* **2008**, *120*, 167–175.
(41) Prasad, P. N.; Willians, D. J. *Introduction to Nonlinear Optical Effects in Molecules and Polymers*; John Wiley & Sons: New York, 1991.
(42) Bonin, K. D.; McIlrath, T. J. *J. Opt. Soc. Am. B* **1984**, *1*, 52–55.
(43) Sadler, D. M. *Nature* **1987**, *326*, 174–177.
(44) Lois, S.; Flores, J. C.; Lè re-Porte, J. P.; Serein-Spirau, F.; Moreau, J. J. E.; Miqueu, K.; Sotiropoulos, J. M.; Baylere, P.; Tillard, M.; Belin, C. *Eur. J. Org. Chem.* **2007**, *24*, 4019–4931.
(45) Chin, R. P.; Shen, Y. R.; Petrovakoch, V. *Science* **1995**, *270*, 776–778.
(46) Birge, R. R.; Bennett, J. A.; Pierce, B. M.; Thomas, T. M. *J. Am. Chem. Soc.* **1978**, *100*, 1533–1539.
(47) Mongin, O.; Porres, L.; Charlot, M.; Katan, C.; Blanchard-Desce, M. *Chem.—Eur. J.* **2007**, *13*, 1481–1498.
(48) Zheng, S. J.; Leclercq, A.; Fu, J.; Beverina, L.; Padilha, L. A.; Zojer, E.; Schmidt, K.; Barlow, S.; Luo, J. D.; Jiang, S. H.; et al. *Chem. Mater.* **2007**, *19*, 432–442.
(49) Day, P. N.; Nguyen, K. A.; Pachter, R. *J. Phys. Chem. B* **2005**, *109*, 1803–1814.
(50) Rubio-Pons, O.; Luo, Y.; Agren, H. *J. Chem. Phys.* **2006**, *124*, 094310.
(51) Vivas, M. G.; Piovesan, E.; Silva, D. L.; Cooper, T. M.; De Boni, L.; Mendonca, C. R. *Opt. Mat. Exp.* **2011**, *1*, 700–710.
(52) Yi, Y. P.; Zhu, L. Y.; Shuai, Z. *J. Chem. Phys.* **2006**, *125*, 164505.